SLENDER BODY THEORY FOR THREE-DIMENSIONAL BOUNDARY-LAYER INDUCED POTENTIAL FLOWS

Stanley G. Rubin, et al

Poiytechnic Institute of Brooklyn

Prepared for:

Air Force Office of Scientific Research

August 1973

DOCUMENT CONTROL DATA - R & D AD773362

(Security classification of title, body of abstract and indexing annotation must be entered when the overall report is classified)

1. ORIGINATING ACTIVITY (Corporate author)
POLYTECHNIC INSTITUTE OF BROOKLYN
DEPT. OF AEROSPACE ENGRG. & APPLIED MECHANICS
ROUTE 110, FARMINGDALE, NEW YORK 11735

2a. REPORT SECURITY CLASSIFICATION
UNCLASSIFIED

2b. GROUP

3. REPORT TITLE
SLENDER BODY THEORY FOR THREE-DIMENSIONAL BOUNDARY LAYER INDUCED POTENTIAL FLOWS

4. DESCRIPTIVE NOTES (Type of report and inclusive dates)
Scientific Interim

5. AUTHOR(S) (First name, middle initial, last name)
STANLEY G RUBIN
FRANK J MUMMOLO

6. REPORT DATE	7a. TOTAL NO. OF PAGES	7b. NO. OF REFS
August 1973	28 34	13

8a. CONTRACT OR GRANT NO.	9a. ORIGINATOR'S REPORT NUMBER(S)
AFOSR 70-1843	PIBAL REPORT NO. 73-16
b. PROJECT NO. 9781-01	
c. 61102F	9b. OTHER REPORT NO(S) (Any other numbers that may be assigned this report)
d. 681307	AFOSR - TR - 74 - 0039

10. DISTRIBUTION STATEMENT
Approved for public release; distribution unlimited.

11. SUPPLEMENTARY NOTES	12. SPONSORING MILITARY ACTIVITY
TECH, OTHER	AF Office of Scientific Research-NAM 1400 Wilson Boulevard Arlington, Virginia 22209

13. ABSTRACT

The application of slender body theory for the evaluation of three-dimensional boundary layer induced surface crossflow and streamwise velocities is considered. The method is applicable to sub- and supersonic flows when small perturbation theory applies, and when the Reynolds number is large so that the thin boundary layer approximation is valid. The resulting potential problem is, in general, reduced to a two-dimensional consideration of the flow over an expanding cylinder with porous boundary conditions. As a model problem, the induced surface velocities are determined for the constant density flow over a body with constant elliptical cross-section. The limiting solutions for a flat plate of finite span and a near circular cross-section are obtained in a simple anlalytic form. In the former case, within the limitations of slender body theory, the results are in exact agreement with the complete three-dimensional solution for this geometry.

DD FORM 1 NOV 65 1473

UNCLASSIFIED
Security Classification

KEY WORDS	LINK A		LINK B		LINK C	
	ROLE	WT	ROLE	WT	ROLE	WT
SLENDER BODY THEORY						
THREE-DIMENSIONAL POTENTIAL FLOW						
THREE-DIMENSIONAL VISCOUS-INVISCID INTERACTIONS						
TRANSVERSE CURVATURE EFFECTS						

UNCLASSIFIED

Security Classification

SLENDER BODY THEORY FOR THREE-DIMENSIONAL BOUNDARY LAYER INDUCED POTENTIAL FLOWS

by

Stanley G. Rubin and Frank J. Mummolo

This research was supported by the Air Force Office of Scientific Research under Grant No. AFOSR 70-1843 and Modification No. AFOSR 70-1843A, Project No. 9781-01.

POLYTECHNIC INSTITUTE OF BROOKLYN

Department

of

Aerospace Engineering and Applied Mechanics

August 1973

PIBAL Report No. 73-16

TABLE OF CONTENTS

LIST OF ILLUSTRATIONS

SLENDER BODY THEORY FOR THREE-DIMENSIONAL BOUNDARY LAYER INDUCED POTENTIAL FLOWS[†]

By Stanley G. Rubin[‡] and Frank J. Mummolo[*]
Polytechnic Institute of Brooklyn, Farmingdale, New York

ABSTRACT

The application of slender body theory for the evaluation of three-dimensional boundary layer induced surface crossflow and streamwise velocites is considered. The method is applicable to sub- and supersonic flows when small perturbation theory applies, and when the Reynolds number is large so that the thin boundary layer approximation is valid. The resulting potential problem is, in general, reduced to a two-dimensional consideration of the flow over an expanding cylinder with porous boundary conditions. As a model problem, the induced surface velocities are determined for the constant density flow over a body with constant elliptical cross-section. The limiting solutions for a flat plate of finite span and a near circular cross-section are obtained in a simple analytic form. In the former case, within the limitations of slender body theory, the results are in exact agreement with the complete three-dimensional solution for this geometry.

[†]This research is sponsored by the Air Force Office of Scientific Research, Office of Aerospace Research, USAF, under Grant No. AFOSR 70-1843, Project No. 9781-01.

[‡]Associate Professor of Aerospace Engineering.

[*]Research Assistant, Dept. of Aerospace Engineering and Applied Mechanics.

1. Introduction

Three-dimensional boundary layer induced crossflow analyses, in particular on surfaces with locally large or even infinite transverse curvature,* belong to a class of problems for which the current state-of-the-art is still inadequate. Only a limited group of analyses, for very specific geometries, is presently available. These include the quarter plate investigations of Stewartson and Howarth (1960) and Stewartson (1961), and the cruciform studies of Rubin (1966), Pal and Rubin (1971) and Rubin and Grossman (1971).

One of the difficulties associated with the determination of boundary layer interactions of this type is the complexity of the three-dimensional potential problem that arises when the displacement induced flow field is to be evaluated. From this potential flow solution, boundary layer induced streamwise velocities and crossflows are determined. With a systematic application of singular perturbation methodology, the induced velocity distributions along the surface become the necessary asymptotic matching conditions for the crossflow boundary layer analysis, as well as for higher order boundary layer considerations. Special care must be exercised at points of large transverse curvature such as the edge or corner intersection line. In these boundary regions, crossflow diffusion is important even for the lowest order theory.

Since the crossflow and second-order boundary layer analyses require, as asymptotic boundary conditions, only the potential velocities evaluated along the surface, the slender body theory of Munk, Jones and Ward (M-J-W), for many years a powerful

---

*i.e., when the local cross-sectional curvature multiplied by the local boundary layer thickness is O(1) or larger.

approximation in inviscid aerodynamic theory, is adapted here for application to high Reynolds number viscous flows.

When considering parallel flows over bodies with locally small longitudinal curvature, the concepts of small perturbation theory apply (Sears (1960)). The governing equations in terms of a velocity potential φ reduce to the simplified linear Prandtl-Glauert equation for sub- or supersonic flow;

$$\beta^2 \varphi_{ss} + \varphi_{yy} + \varphi_{zz} = 0 \tag{1}$$

where s denotes the stream direction, y and z the cross plane directions (see, figure 1); $\beta^2=1-M_\infty^2$; M_∞^2 is the stream Mach number. For incompressible flow $\beta^2=1$ and (1) is exact.

For slender bodies with slowly varying cross-sectional areas, the M-J-W theory specifies that in the vicinity of the surface, a first approximation for (1) reduces to

$$\varphi_{yy} + \varphi_{zz} = 0 \tag{2}$$

so that the solution of (1) is of the form

$$\varphi(s,y,z) = \hat{\varphi}(y,z;s) + b_o(s) \tag{3}$$

where

$$b_c(s) = \frac{S'(s)}{4\pi} \ln \frac{\beta^2}{4s(\ell-s)} - \frac{1}{4\pi} \int_o^\ell \frac{S'(x)-S'(s)}{|s-x|} dx \quad (M_\infty < 1) \tag{4a}$$

$$b_o(s) = \frac{S'(s)}{2\pi} \ln \frac{\beta}{2s} - \frac{1}{2\pi} \int_o^s \frac{S'(x)-S'(s)}{s-x} dx \quad (M_\infty > 1) \tag{4b}$$

S(s) denotes the local cross-sectional area of a body of length ℓ, see Ward (1955).

Therefore, the original three-dimensional potential problem (1) is replaced by a much simpler two-dimensional problem (2) for the induced flow near the surface. This remarkable simplification allows for the solution of a wide variety of aerodynamic problems for which the general potential solution can only be represented

by quadratures.

In view of the fact that it is precisely the surface velocities that are required for evaluating the induced cross flow and higher order boundary layers, the M-J-W procedure lends itself to the evaluation of the boundary layer induced potential flow. A complete discussion of this procedure as well as application to an elliptic cylinder is presented in this paper. Consideration of specific cross flow boundary layers as well as the general effects of large transverse curvature in boundary layer theory will be the subject of future considerations.

2. Formulation

Consider the uniform flow over a cylindrical body of arbitrary cross section at zero incidence.* Local body slopes are assumed to be small so that the uniform flow is only slightly disturbed by the presence of the body and small perturbation theory as prescribed by (1) applies. Furthermore, variations in cross-sectional area are also assumed to be small so that near the surface the M-J-W theory with (2) and (3) apply for the inviscid potential problem.

The Reynolds number $R_a = Ua/\nu$ based on freestream values and a typical body dimension a is assumed to be large so that a thin boundary layer develops over the body. Therefore, the boundary layer induced potential flow is also governed by (1) and in view of the linearity of (1) and the small disturbance boundary conditions,

*The effects of small angles of attack or yaw, while not precluded by the analysis, are not specifically considered in this paper.

Sears (1960), the viscous and geometric problems can be treated independently to first-order in $Re^{-\frac{1}{2}}$ and τ, a characteristic thickness ratio.

The geometric inviscid problem has been discussed in great detail, see Ward (1955), so that we shall confine our remarks to the boundary layer induced flow over cylinders of constant cross-sectional area, $\tau=0$. For these geometries, provided that the transverse curvature of the cylinder is nowhere large, a Blasius boundary layer with thickness $\delta \sim s^{\frac{1}{2}}$ forms along the generators of the cylinder, Cooke (1957). Regions with locally large or infinite transverse curvature (boundary regions), or the flow near a blunted nose cap attached to the cylinder, must be treated separately by local singular perturbation analyses, see Rubin (1966) and Van Dyke (1964). For the downstream flow considered here, the shape of the nose is immaterial, see Seban and Bond (1951).

It should be emphasized that the method to be presented herein requires only that viscous displacement effects are small, i.e., thin boundary layers. The analysis is applicable to geometries with non-constant cross-sections provided the longitudinal curvature is small, $\tau<<1$. For these cases it is assumed that the boundary layer solution is determinable. For slender bodies the inviscid perturbation streamwise velocity is of order $\tau^2 \ln \tau$. If we accept an error of this order for the boundary layer formulation, the lowest-order solution always reduces to the Blasius function.

The surface boundary layer perturbs the outer potential flow in much the same way as streamwise variations in body cross-sectional area. The viscous displacement induces crossflows and higher order streamwise velocities. When evaluated at the surface, these velocities serve as asymptotic matching conditions for the boundary layer determinations. The effective displacement body remains slender, so that the M-J-W theory with (2-4) should apply near the surface. S(s) can now be interpreted as the modified body cross-section, taken to include the displacement boundary layer.

For a general slender body at zero incidence the familiar inviscid M-J-W slender body formulation reduces to a two-dimensional problem (2) for the flow over an expanding body. The boundary condition applied at the surface relates the normal gradient of the potential function φ to the local streamwise body slope. For the boundary layer induced potential flow, the slender body theory also leads to a two-dimensional problem (2) for the flow over an expanding body. The boundary values are obtained by asymptotic matching to the inner boundary layer. For large Re this condition is applied at the surface of the cylinder (see footnote on page 8). In view of the linearity of this potential problem, the complete solution can be obtained by superposition of the geometric and viscous induced flows.

The details of the analysis are presented in the next section where the incompressible viscous flow over a cylinder with constant elliptic cross-section is considered. The complete solution is

described and the axisymmetric and zero thickness limits are obtained. A particularly simple form of the solution results for cross-sections that are nearly circular. The zero thickness limit is compared with the three-dimensional solution obtained from an extension of the quarter-plate analysis of Stewartson and Howarth (1960).

3. Solution For An Elliptic Cylinder

Consider the incompressible flow over a cylinder of constant elliptic cross-section. The generators of the cylinder are taken parallel to the freestream with $\ell \geq s \geq 0$ (figure 1). The Reynolds number based on the semi-major axis is large so that boundary layer theory applies in the usual manner. It is assumed here that the transverse curvature of the cross-section is small with respect to the boundary layer thickness, although in a more general consideration this condition may be violated locally* along discrete generators. This would occur at the ends of a highly eccentric elliptic cross-section or in a limiting case at the edges of a plate of zero thickness. These singular lines diffuse into what are termed boundary regions and must be treated separately (see Stewartson (1961) or Rubin (1966)). To lowest-order, however, the viscous boundary regions do not affect the flow behavior in the adjoining three-dimensional boundary layers or the outer inviscid potential flow.

As stated previously, to lowest-order the boundary layer on a constant area cylinder, downstream of a leading edge or nose

* In small local regions that are of zero thickness as $\nu \to 0$.

region and away from boundary regions, is identical with the constant pressure flat plate boundary layer. Transverse curvature enters only in higher order approximations. This solution, due to Blasius, is well-known, Van Dyke (1964). It is sufficient to note here that the viscous induced displacement velocity v directed normal to the surface has the following asymptotic behavior for large values of the boundary layer variable $\eta=\hat{y}(U/2\nu s)^{\frac{1}{2}}$:

$$\lim_{\eta\to\infty} \frac{v(s,\eta)}{U} \sim \frac{0.860}{R_s^{\frac{1}{2}}} \tag{5}$$

and the displacement thickness Δ^* is given by the relation

$$\Delta^* = 1.72s/R_s^{\frac{1}{2}} \tag{6}$$

where $R_s=Us/\nu$; U denotes the undisturbed stream and $(\hat{y},\lambda,s)$ are the surface normal, azimuthal and streamwise coordinates, respectively, defined in figure 1.

For large Reynolds numbers, $R_s>>1$, the inviscid outer flow is only slightly perturbed by the formation of the thin boundary layer on the surface and therefore the solution for the incompressible displacement induced potential flow can be determined from (1) with $M_\infty=0$.

A far field velocity decay condition

$$\nabla\phi\to 0 \tag{7a}$$

applies at large distances from the body and a smooth match with the inner boundary layer must be prescribed. This surface matching condition is specified by

$$\lim_{\hat{y}\to 0} \bar{n}\cdot\nabla\phi(s,\hat{y},\lambda)=\lim_{\eta\to\infty} v/U \sim 0.860/R_s^{\frac{1}{2}} \quad * \tag{7b}$$

*When the largest cross-section dimension is of the order of the displacement thickness, the boundary condition cannot be applied at $\hat{y}=0$, but only at $\hat{y}=\Delta^*$. This point will be illustrated in a later example.

In most cases the boundary condition (7b) can be imposed directly on the surface $\hat{y}=0$; however, the resulting three-dimensional potential problem is still a formidable one. This is particularly true with complex body cross-sections. To the authors' knowledge, three-dimensional boundary layer induced potential flows have been calculated only in a few cases with simple geometries, e g., the quarter-plate of Stewartson (1961) and the cruciform of Rubin (1966). In the former case only integrated surface conditions were obtained.

In order to generate surface values for application in higher order boundary layer theory and to evaluate the induced surface cross flow, the three-dimensional potential problem can be reduced to a quasi-two-dimensional form with the M-J-W slender body approximation. The displacement body prescribed by (6) describes a slender body, and the governing equation (2) with (3) and (4) applies. As stated previously, S(s) denotes the cross-sectional area of the body plus displacement thickness.*

In general, the solution of (2) satisfying (7) can be investigated with conformal mapping techniques. However, for the elliptic cross-section considered here, it is convenient to transform to an elliptic coordinate frame in which the general solution is of the form

$$\hat{\varphi} = a_o(s)\xi + c_o(s) + \sum_{n=1}^{\infty} a_n(s)e^{-n\xi}\cos n\theta \qquad (8)$$

*It should be noted that with $S'(s)\sim s^p$, the integral in (4a) is divergent for semi-infinite bodies ($\ell\to\infty$) with $p>0$; however, the perturbation velocities depend on $b_o'(s)$ and are well-defined for $p>0$.

where (ξ,ϑ) are elliptic coordinates, figure 2, defined by

$$z=c\cosh\xi\cos\vartheta \tag{9a}$$

$$y=c\sinh\xi\sin\vartheta \tag{9b}$$

$$r^2=y^2+z^2 \quad ; \quad \omega=\tan^{-1}(y/z) \tag{9c}$$

$$\xi=\ln\left(\frac{r}{c}\right)+\tfrac{1}{2}\ln\left\{1+\left[\left(1-\frac{c^2}{r^2}\right)^2+4\left(\frac{c}{r}\right)^2\sin^2\omega\right]^{\frac{1}{2}}+\left[1-\left(\frac{c^2}{r^2}\right)\cos 2\omega+\left\{\left(1-\frac{c^2}{r^2}\right)^2+4\left(\frac{c^2}{r^2}\right)\sin^2\omega\right\}^{\frac{1}{2}}\right)\right]^{\frac{1}{2}}\Bigg\} \tag{9d}$$

and $c^2=a^2-b^2$, $e=c/a=(\cosh\xi_o)^{-1}$, where a and b are the semi-major and minor axes, respectively, and e is the eccentricity.

The boundary condition (7b) becomes

$$\lim_{\xi\to\xi_o}\left[c(\cosh^2\xi-\cos^2\vartheta)^{\frac{1}{2}}\right]^{-1}\frac{\partial\varphi}{\partial\xi}(\xi,\vartheta;s)=(0.860/R_a^{\frac{1}{2}})(a/s)^{\frac{1}{2}}=\frac{d\Delta^*}{ds} \tag{10}$$

where the surface is denoted by the ellipse $\xi=\xi_o$.

The coefficient a_n are defined by

$$a_o=\frac{1}{2\pi}\int_o^{2\pi}\frac{\partial\varphi}{\partial\xi}(\xi_o,\vartheta;s)\,d\vartheta \tag{11a}$$

$$a_n=\frac{-2e^{-n\xi_o}}{n\pi}\int_o^{\pi}\frac{\partial\varphi}{\partial\xi}(\xi_o,\vartheta;s)\cos n\vartheta\,d\vartheta \tag{11b}$$

where $\frac{\partial\varphi}{\partial\xi}(\xi_o,\vartheta,s)$ is determined from (10).

The coefficient $2\pi a_o$ can be shown to represent the derivative of the "effective" cross-sectional surface area of the ellipse denoted here as $S'(s)$.[+] This result is exact when the boundary condition (7b) is satisfied at the displacement surface and in certain limiting cases where the boundary condition is transferred to the surface (10), e.g., a circular cross section or flat plate. In general, when the boundary condition is transferred to the surface,

[+]This result can easily be proven by a mass conservation argument.

as given by (10), a_o differs from $S'(s)$ by a term of order Δ^{*2}. This difference is negligible in the present analysis but would reappear if higher order solutions for the outer inviscid flow were considered. Therefore, the surface area terms $S'(s)$ in (4) are represented by

$$S'(s)=2\pi a_o=\left\{\lim_{\xi\to\xi_o}\int_o^{2\pi} c(\cosh^2\xi-\cos^2\theta)^{\frac{1}{2}}d\theta\right\}\frac{d\Delta^*}{ds} \tag{12}$$

or

$$S'(s)=4a\ E(\frac{\pi}{2},e)\ \frac{d\Delta^*}{ds} \tag{12a}$$

where E is a complete elliptic integral of the second kind, defined in Gradshteyn and Ryzhik (1965), p. 909.

Some limiting cases are

(1) For a circle of radius a: $c\to 0$, $c\cosh\xi_o\to a$, so that

$$S'(s)=2\pi a\ \frac{d\Delta^*}{ds} \tag{12b}$$

(2) For a circle of radius $a=O(\Delta^*)$: $c\to 0$, $\lim_{\xi\to\xi_o} c\cosh\xi\to a+\Delta^*$ and (12) gives

$$S'(s)=2\pi(a+\Delta^*)\ \frac{d\Delta^*}{ds} \tag{12c}$$

This case is not physically meaningful, as the ratio $a/\Delta^*=O(1)$ and the Blasius solution is no longer appropriate; however, it provides an interesting limit when $a\to 0$ because the body is then reduced to a paraboloid of revolution. The exact solution for this problem was given by Van Dyke (1964).

(3) For a flat plate of span 2a: $b\to 0$, $c\to a$, $\xi_o\to 0$ and (12a) gives

$$S'(s)=4a\ \frac{d\Delta^*}{ds} \tag{12d}$$

The coefficient $c_o(s)$ in (8) is defined so that the expressions (4) obtained by Ward (1955) are applicable in that form, see Kahane and Solarski (1953).

$$c_o(s) = a_o(s) \ln \frac{c}{2} \tag{12e}$$

Therefore, with (4), (10-12e), and noting that odd coefficients a_n vanish, the solution for φ becomes

$$\varphi(s,\xi,\theta) = \frac{S'(s)}{2\pi}(\xi+\ln\frac{c}{2})+b_o(s)+$$

$$\frac{-1.72c}{\pi R_s^{1/2}} \sum_{n=1}^{\infty} \frac{e^{-2n(\xi-\xi_o)}}{n} \left\{\int_o^{\pi/2} (\cosh^2\xi_o-\cos^2\theta)^{1/2}\cos 2n\epsilon\, d\theta\right\}\cos 2n\theta \tag{13}$$

The induced velocities at the surface of the ellipse $\xi=\xi_o$ are

$$\frac{u}{U} = \varphi_s = \frac{-0.860}{\pi R_a^{1/2}}\left(\frac{a}{s}\right)^{3/2}\left[\left\{\ln\left(\frac{a}{16s}\right)(1+\sqrt{1-e^2})+2\right\}E\left(\frac{\pi}{2},\epsilon\right)+\right.$$

$$\left.-\sum_{n=1}^{\infty}\frac{\cos 2n\theta}{n}\left\{\int_o^{\pi/2}\sqrt{1-e^2\cos^2\beta}\,\cos 2n\beta\, d\beta\right\}\right] \tag{14a}$$

$$\frac{w}{U} = \frac{1}{a}(1-e^2\cos^2\theta)^{-1/2}\varphi_\theta =$$

$$\frac{3.44}{\pi R_a^{1/2}}\left(\frac{a}{s}\right)^{1/2}\sum_{n=1}^{\infty}\frac{\sin 2n\theta}{(1-e^2\cos^2\theta)^{1/2}}\int_o^{\pi/2}(1-e^2\cos^2\beta)^{1/2}\cos 2n\beta\, d\beta \tag{14b}$$

Expressions (14a) and (14b) represent the boundary layer induced velocities evaluated at the surface of a body having a constant elliptic cross-section. The crossflow boundary layer and first order correction to the streamwise Blasius profile require these values as outer matching conditions. Previous boundary layer analyses of transverse curvature effects on cylinders of circular and more general cross-section have erroneously neglected these

displacement induced boundary conditions, e.g., Cooke (1957), Seban and Bond (1951). A discussion of the errors arising from the neglect of these displacement effects for the case of a circular cylinder was given by Van Dyke (1971). The complete boundary layer analysis is currently under investigation. For the remainder of the present paper, the solutions (14) for the induced velocities will be discussed for different eccentricities; the limiting circular and flat plate results will be obtained for comparison with known exact solutions. This will establish the validity of the M-J-W theory to boundary layer problems and serve as a model for examinations of more complex cross-sections where exact three-dimensional solutions are not presently available.

4. Flat Plate of Finite Span

The flat plate represents the simplest geometry for which displacement induced crossflows appear. With the formulation presented herein, the surface velocities can be evaluated from the general solution of section 3 by a direct limiting process $\xi_o \to 0$, $c \to a$. The solution for this geometry is also easily obtainable by the appropriate application of Green's functions: two-dimensional for the slender body theory discussed here and three-dimensional for the classical formulation. This latter approach has been considered by Stewartson and Howarth (1960) for a quarter-infinite flat plate and is readily extended to the finite-span case.

A. Three-Dimensional Solution

Consider a plate of span 2a as shown in figure 3. Away from the side edge boundary regions, a Blasius boundary layer forms on the plate and the three-dimensional displacement induced potential problem becomes

$$\varphi_{ss} + \varphi_{yy} + \varphi_{zz} = 0$$

with $\nabla\varphi \to 0$ as $(y^2+z^2)^{\frac{1}{2}} \to \infty$

and $(\varphi_y)_{y=0} = 0.860 U R_s^{-\frac{1}{2}} \operatorname{sgn} y; \quad |z|<a, \; s>0$

and $(\varphi_y)_{y=0} = 0$ elsewhere.

Following Stewartson and Howarth (1960), the solution is given by

$$-2\pi\varphi(s,y,z) = \frac{0.860U}{R_s^{\frac{1}{2}}} \int_0^{\infty} \frac{dX}{X^{\frac{1}{2}}} \int_{-a}^{a} \frac{d\xi}{[(\xi-z)^2+y^2+(X-s)^2]^{\frac{1}{2}}}$$

It follows that

$$\frac{v}{U} = \frac{-0.860}{2\pi} \sqrt{\frac{\nu}{U}} \int_0^{\infty} \frac{dX}{X^{\frac{1}{2}}} \int_{-a}^{a} \frac{(\xi-z)\,d\xi}{[(\xi-z)^2+y^2+(X-s)^2]^{3/2}}$$

$$\frac{u}{U} = \frac{-0.860}{2\pi} \sqrt{\frac{\nu}{U}} \int_0^{\infty} \frac{(X-s)\,dX}{X^{\frac{1}{2}}} \int_{-a}^{a} \frac{d\xi}{[(\xi-z)^2+y^2+(X-s)^2]^{3/2}}$$

On the plate y=0, with a/s<<1, the crossflow velocity takes the form

$$\left(\frac{w}{U}\right)_{y=0} = \frac{-0.860}{\pi R_s^{\frac{1}{2}}} \log\left[\frac{a-z}{a+z}\right] \qquad (15a)$$

Along the plate centerline, y=0, z=0 and with a/s<<1, the streamwise perturbation becomes

$$\left(\frac{u}{U}\right)_{y=0=z} = \frac{-0.860}{\pi R_s^{1/2}}\left[\frac{a}{s}\left(\log\frac{a}{8s} + 1\right)\right] \qquad (15b)$$

while at the plate edge we obtain

$$\left(\frac{u}{U}\right)_{\substack{y=0\\z=a}} = \frac{-0.860}{\pi R_a^{1/2}}\left(\frac{a}{s}\right)^{3/2}\left[\log\left(\frac{a}{4s}\right) + 1\right] \qquad (15c)$$

B. Flat Plate as the Limit of the Elliptic Cylinder with M-J-W Theory

This limit can be obtained from (14) by setting $\xi_o \equiv 0$ and noting that from (12d) that

$$a_o(s) = \frac{2a}{\pi}\frac{d\Delta^*}{ds} = \frac{S'(s)}{2\pi}$$

The streamwise perturbation velocity (14a), on the plate centerline $\theta=\pi/2$ becomes

$$\left(\frac{u}{U}\right)_{y=0=z} = \frac{S''}{2\pi}\left[\ln\frac{a}{2} + \sum_{n=1}^{\infty}\frac{(-1)^n}{n(4n^2-1)}\right] + b_o'(s)^*$$

$$= \frac{-0.860}{\pi R_s^{1/2}}\left(\frac{a}{s}\right)\left[\log\frac{a}{8s} + 1\right] \qquad (16)$$

and at the edge (15c) is recovered. See Gradshteyn and Ryzhik (1965), p. 46.

The crossflow on the plate is given by

$$\left(\frac{w}{U}\right)_{y=0} = \frac{-S'(s)}{\pi a|\sin\theta|}\sum_{n=1}^{\infty}\frac{\sin 2n\theta}{4n^2-1}$$

*Here $b_o'(s)$ denotes the derivative of (4a) in the limit $\ell\to\infty$.

It is easily shown that

$$\frac{4}{|\sin\theta|}\sum_{n=1}^{\infty}\frac{\sin 2n\theta}{4n^2-1} = \log\left(\frac{a-z}{a+z}\right)$$

where from (9b) $z=a\cos\theta$. Therefore

$$\left(\frac{w}{U}\right)_{y=0} = \frac{-0.860}{\pi R_s^{\frac{1}{2}}}\log\left(\frac{a-z}{a+z}\right) \tag{17}$$

These results (16) and (17) are in exact agreement with three-dimensional solutions (15).

C. M-J-W Theory for the Flat Plate. Direct Formulation

The slender body solution for the induced velocities on a flat plate can also be determined by direct application of a two-dimensional Green's function. With the governing equation for $\hat{\varphi}(y,z;s)$

$$\hat{\varphi}_{yy} + \hat{\varphi}_{zz} = 0$$

and the boundary conditions

$$\nabla\hat{\varphi} \to 0 \qquad \text{as} \quad (y^2+z^2)^{\frac{1}{2}} \to \infty$$

$$(\hat{\varphi}_y)_{y=0} = \frac{0.860}{R_s^{\frac{1}{2}}}\,\text{sgn}\, y \qquad |z| < a$$

$$(\hat{\varphi}_y)_{y=0} = 0 \qquad |z| > a$$

it follows that

$$2\pi\hat{\varphi} = \frac{0.860}{R_s^{\frac{1}{2}}}\int_{-a}^{a}\log[(X-z)^2+y^2]\,dX$$

Therefore,

$$\frac{w}{U} = \frac{-0.860}{2\pi R_s^{\frac{1}{2}}}\log\left[\frac{(a-z)^2+y^2}{(a+z)^2+y^2}\right] \tag{18}$$

and

$$\left(\frac{u}{U}\right)_{z=0} = \frac{-0.860}{\pi R_s^{\frac{1}{2}}} \left(\frac{a}{s}\right)\left[\log(a^2+y^2)^{\frac{1}{2}} - 1 - \frac{y}{a}\tan^{-1}\frac{a}{y}\right] + b_o'(s) \qquad (19)$$

On the surface y=0 the solutions (15) are recovered for u/U and w/U respectively.

5. Quasi-Axisymmetric Flow

For geometries where the cross-sections are close to circular ($e \ll 1$), the leading terms in an expansion of (14) for small e take a particularly simple form. We find that

$$\left(\frac{u}{U}\right)_{\xi=\xi_o} = \frac{-0.430}{R_a^{\frac{1}{2}}}\left(\frac{a}{s}\right)^{3/2}\left[\left(1-\frac{e^2}{4}\right)\left\{\left(1-\frac{e^2}{4}\right)\ln\left(\frac{a}{8s}\right)+2\right\}+\frac{e^2}{8}\cos 2\theta\right]+O(e^4) \qquad (18a)$$

and

$$\left(\frac{w}{U}\right)_{\xi=\xi_o} = \frac{-0.215}{R_a^{\frac{1}{2}}}\left(\frac{a}{s}\right)^{\frac{1}{2}} e^2 \sin 2\theta + O(e^4) \qquad (18b)$$

where from (12)

$$S'(s) = \frac{1.72\pi a}{R_s^{\frac{1}{2}}}\left(1-\frac{e^2}{4}\right) + O(e^4)$$

The relation

$$\int_o^{\pi/2} \cos^{2m} x \cos 2nx \, dx = \begin{cases} 0 & \text{for } m<n \\ \dfrac{\pi}{2^{2m+1}}\binom{2m}{m-n} & \text{for } m \geq n \end{cases}$$

has been required in obtaining (18) and is useful if additional terms in the expansion are desired. The series in (14) reduce to n terms for the e^{2n} coefficient. The expressions (18) are presented here as limiting velocities, as $e \to 0$, for the general solutions with elliptic cross-section to be discussed in the following section. The axisymmetric solutions (e=0) have previously been obtained by Van Dyke (1970), who also discussed the second order boundary layer and corrected an earlier paper by Seban and Bond (1951).

Finally, the special limiting case of a needle $a \to 0$, $e \to 0$ leads to the flow over a slender paraboloid of revolution. While the Blasius boundary layer is incorrect in this limit, (see Glauert and Lighthill (1955)), the exact solution for a paraboloid is known and provides an additional check on the theory, Van Dyke (1964). With the cylindrical radius defined by

$$R_o(s) = (2\epsilon^2 s)^{\frac{1}{2}}$$

Van Dyke has shown that

$$\varphi = \frac{\epsilon^2}{2} \log(r^2/2\epsilon^2 s)$$

and

$$\frac{u}{U} = -\epsilon^2/2s \tag{19}$$

From (4) and (14a), with (12b), we obtain

$$\frac{u}{U} = b_o'(s) = -(0.860)^2 R_s^{-1} \tag{20}$$

With the cylindrical radius set equal to the effective body radius or displacement thickness Δ^* from (6), we find that (19) and (20) are identical.

6. Elliptic Cylinder

The flow properties at the surface of a cylinder of elliptic cross-section with arbitrary eccentricity e have been determined by numerical evaluation of an appropriate number of terms in the series solutions (14). The integrals in (14) can be expressed by means of recursion relations in terms of elliptic integrals of the first and second kind, see Gradshteyn and Ryzhik (1965). It was more convenient to evaluate the integrals directly by numerical integration. A three-point Simpson's rule having a nominal error of order h^4

was used;h represents the grid apacing. As n increases, the integrand exhibits rapid oscillations and an increased number of mesh points are required. In order to maintain a fixed error, twelve intervals were always located between the zeros of $\cos 2n\theta$ so that 24N+1 points result for n=N.

The number of terms N required to achieve a specified degree of accuracy increases sharply as e→1. The summation was terminated when percentage differences in the sum S and S+5 terms were less than 10^{-10}. The singular behavior in the flat plate limit and in particular near the side edge is not unexpected. For e=1 a logarithmic singularity in the crossflow velocity (14b) appears at the edge, while for e<1, w→0. Also, the asymptotic form of the integrals in (14) shows that e=1 is a singular limit, since

$$\lim_{n\to\infty} \int_0^{\pi/2} \frac{}{\sqrt{1-e^2\cos^2\theta}} \cos 2n\theta d\theta \sim \begin{cases} o(A(e))n^{-M} & \text{for any finite } M>0 \quad (e<1) \\ -(4n^2-1)^{-1} & \text{for } e=1 \end{cases}$$

The asymptotic form for e=1 is also obvious from the exact solution (15a).

The numerical solutions for the crossflow velocity are depicted in figure 4 and confirm the asymptotic predictions. Note the large increase in the maximum number of terms N required for the series solution as e→1. For e=0.999, the solution closely follows the flat plate logarithmic behavior before falling rapidly near the edge. The solution exhibits boundary layer behavior near the edge, with the peak crossflow velocity approaching the edge as e→1. The maximum number of terms required for the series summation generally occurs at a location corresponding to the peak

w value. A boundary region forms near the edge and the three-dimensional viscous flow must be reevaluated.

Similar behavior for the streamwise velocity perturbation is shown in figure 5. While the streamwise velocity distribution is continuous as e→1, the velocity gradient also exhibits a logarithmic singularity. Also depicted on the figures 4 and 5 are solutions for several values of e between zero and one. The simple quasi-axisymmetric expansions for $e<<1$ are given by (18a) and (18b) and are shown in figures 6 and 7. The one term expansions agree quite well with the numerical solutions for $e \leq 0.25$.

7. Summary

When one attempts to analyze the perturbation velocities, and in particular the cross flows, induced by thin boundary layers on three-dimensional geometries, a difficult potential problem results. To date, there are only a minimum number of such exact solutions available. When considering the flow over thin bodies, it has been shown herein that slender body theory, for many years a powerful tool of classical aerodynamics, can be adapted for the determination of boundary layer induced flows. In essence, the potential problem is reduced to the consideration of a two-dimensional flow over an expanding body with porous boundary conditions. This results in a considerable simplification.

The solutions are valid near the body surface and provide insight into the types of crossflows generated by three-dimensional

configurations, as well as supplying asymptotic matching conditions for higher-order boundary layer theory. These displacement induced velocity boundary conditions have generally been neglected in previous perturbation analyses dealing with transverse curvature effects on boundary layer behavior.

The constant density flow over a cylinder of constant elliptical cross-section has been considered. Complete solutions have been obtained in the form of a Fourier series. For the limiting cases of a finite span flat plate or near circular geometry, simplified analytic forms have been obtained. The surface solutions for the plate are in perfect agreement with the exact three-dimensional result obtained by a simple extension of the method of Stewartson and Howarth (1960).

In the general case, a peak cross flow velocity is predicted. The location of this maximum moves toward the side region of the ellipse as the eccentricity e→1. In this limit, the crossflow exhibits a logarithmic behavior, corresponding to the flat plate solutions, up to the peak location and then falls rapidly to zero at the symmetry line. For e→1, the application of a Blasius boundary condition near the edge is incorrect, as transverse curvature is quite large there. Further study will have to consider the side edge flow more exactly in order to determine the precise nature of the developing boundary region where curvature and cross-diffusion effects become important.

8. References

COOKE, J.C. 1957 Quart. Jour. Mech. and Applied Math. 10, 312-321.

GLAUERT, M.B. and LIGHTHILL, M.J. 1955 Proc. Roy. Soc. A 230, 188-203.

GRADSHTEYN, I.S. and RYZHIK, I.M. 1965 Tables of Integrals, Series, and Products. Academic Press.

KAHANE, A. and SOLARSKI, H. 1953 J. Aero. Sci. 20, 513-524.

PAL, A. and RUBIN, S. 1971 Quart. Appl. Math. 29, 91-108.

RUBIN, S. 1966 J. Fluid Mech. 26, 97-110.

RUBIN, S. and GROSSMAN, B. 1971 Quart. Appl. Math. 29, 169-186.

SEARS, W.R. 1960 Small Perturbation Theory. Princeton University Press.

SEBAN, R.A. and BOND, R. 1951 J. Aero. Sci. 18, 671-675.

STEWARTSON, K. 1961 J. Aero. Sci. 28, 1-10.

STEWARTSON, K. and HOWARTH, L. 1960 J. Fluid Mech. 7, 1-21.

VAN DYKE, M. 1964 Perturbation Methods in Fluid Mechanics. Academic Press.

VAN DYKE, M. 1970 Presented at the Sixth U.S. National Congress of Applied Mechanics, Cambridge, Massachusetts.

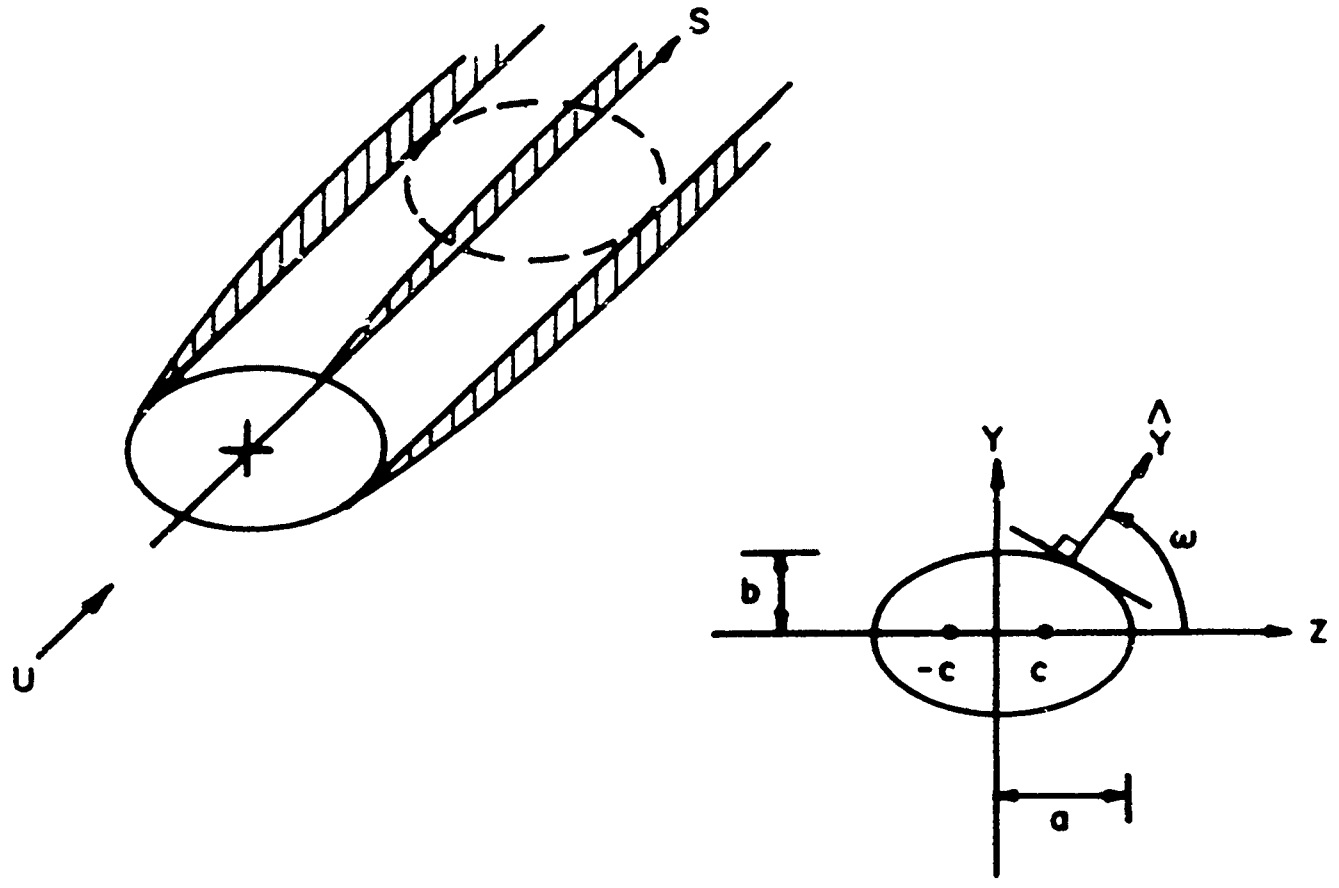

FIG. 1 FLOW GEOMETRY

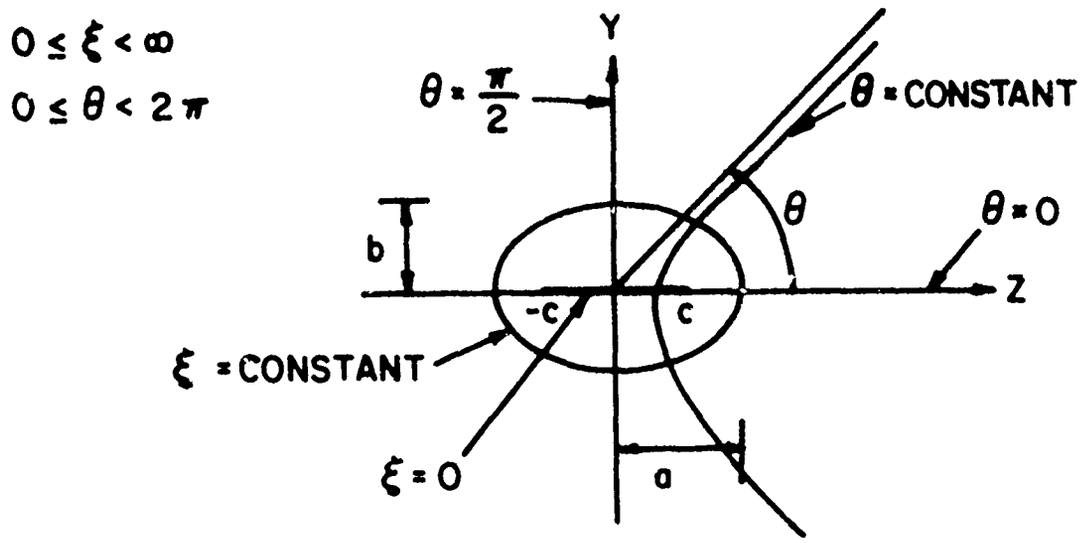

FIG. 2 ELLIPTIC COORDINATES

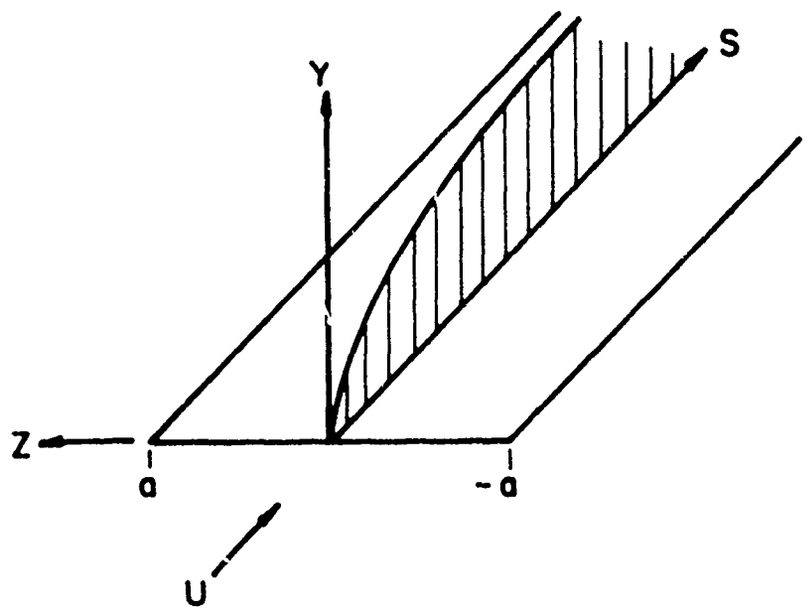

FIG. 3 FLAT PLATE GEOMETRY

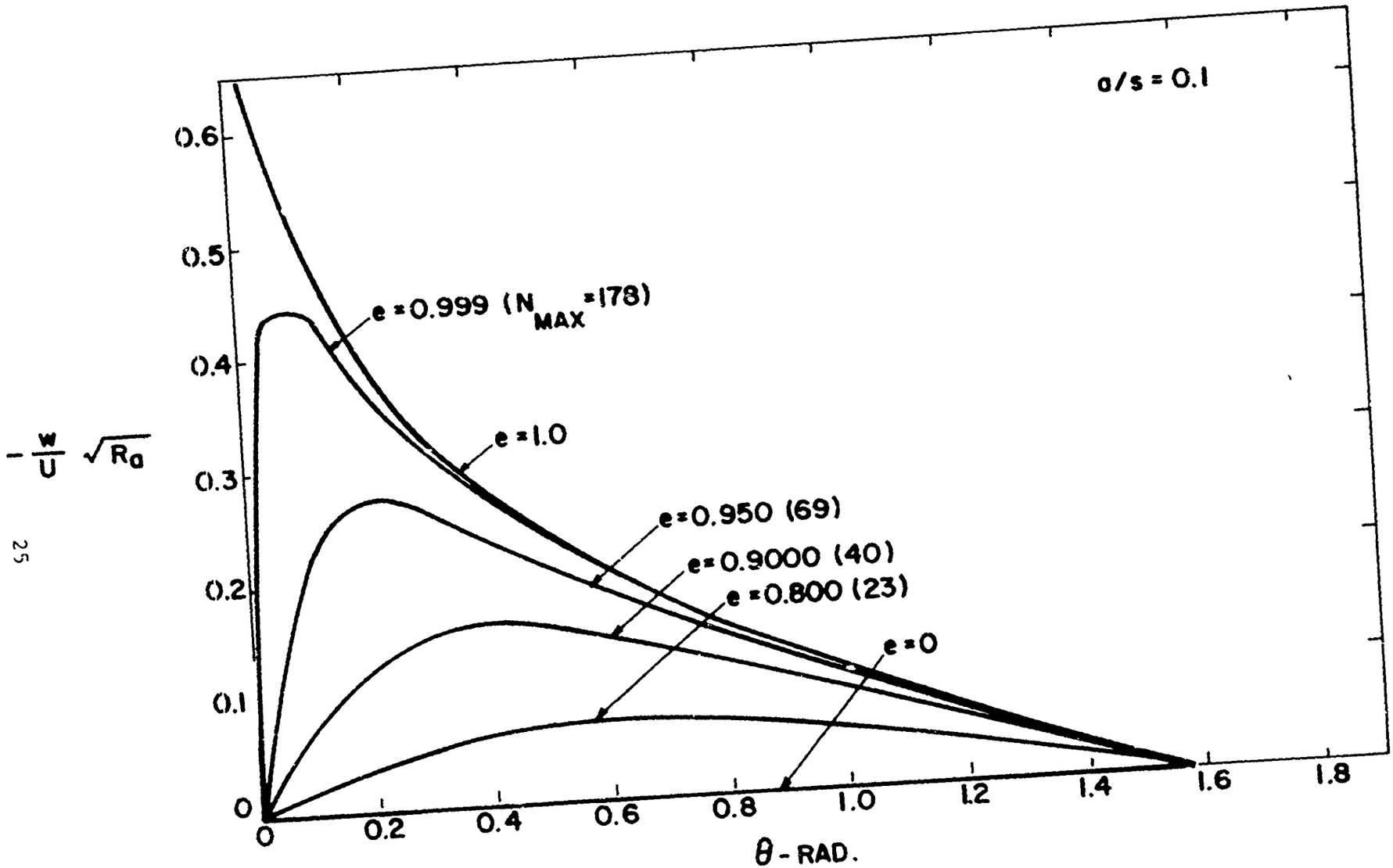

FIG. 4 CROSS FLOW

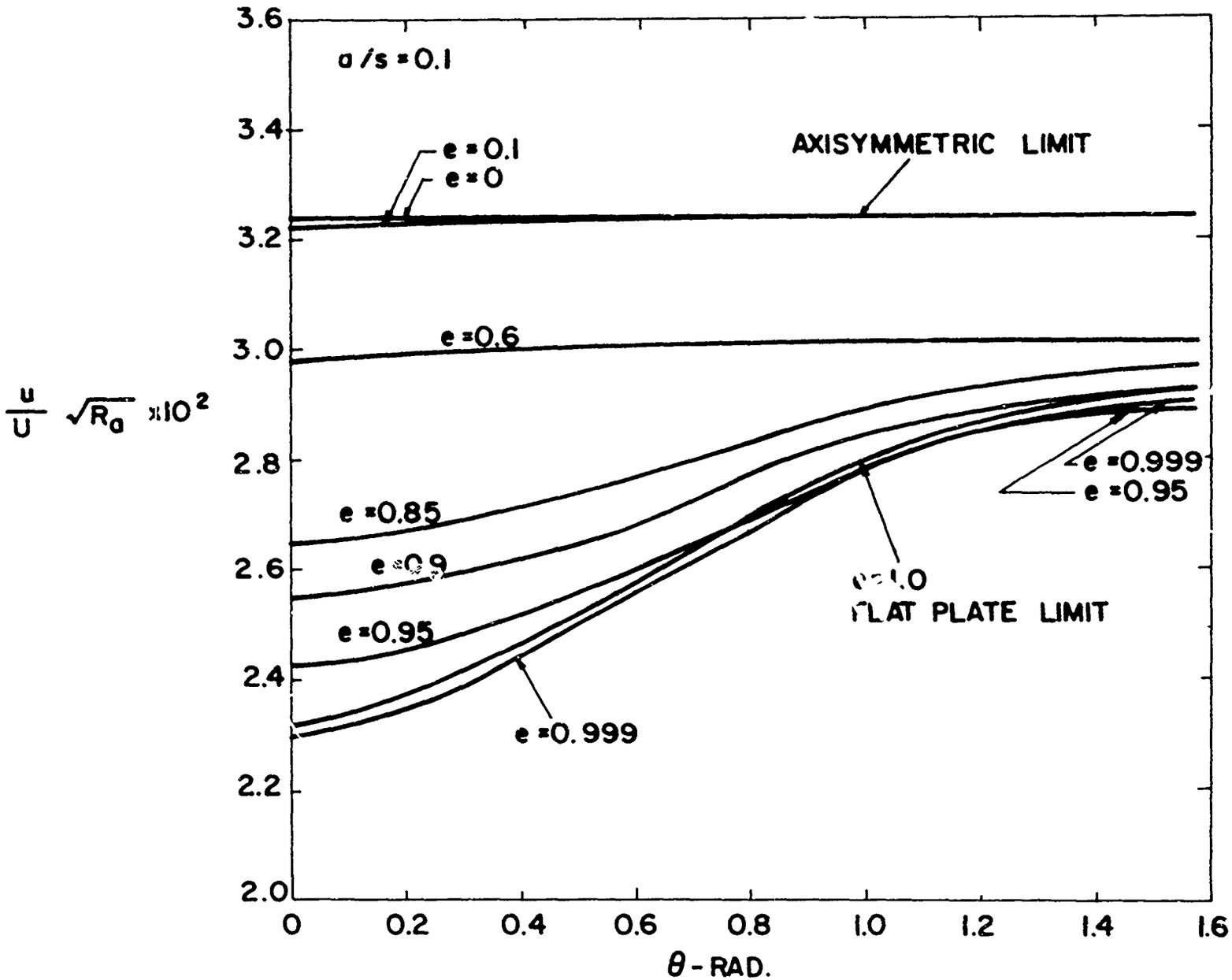

FIG. 5 STREAMWISE PERTURBATION

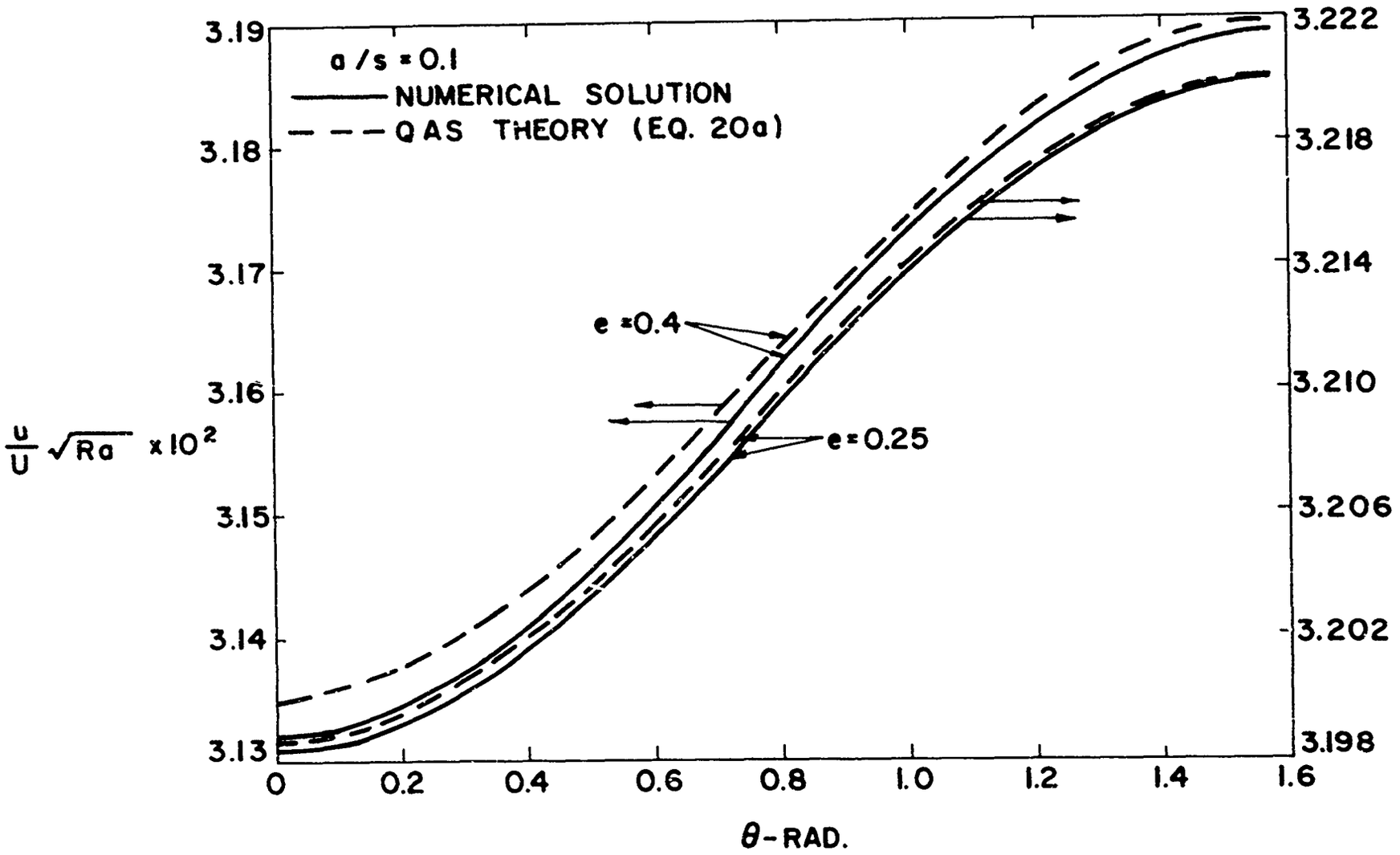

FIG. 6 STREAMWISE PERTURBATION

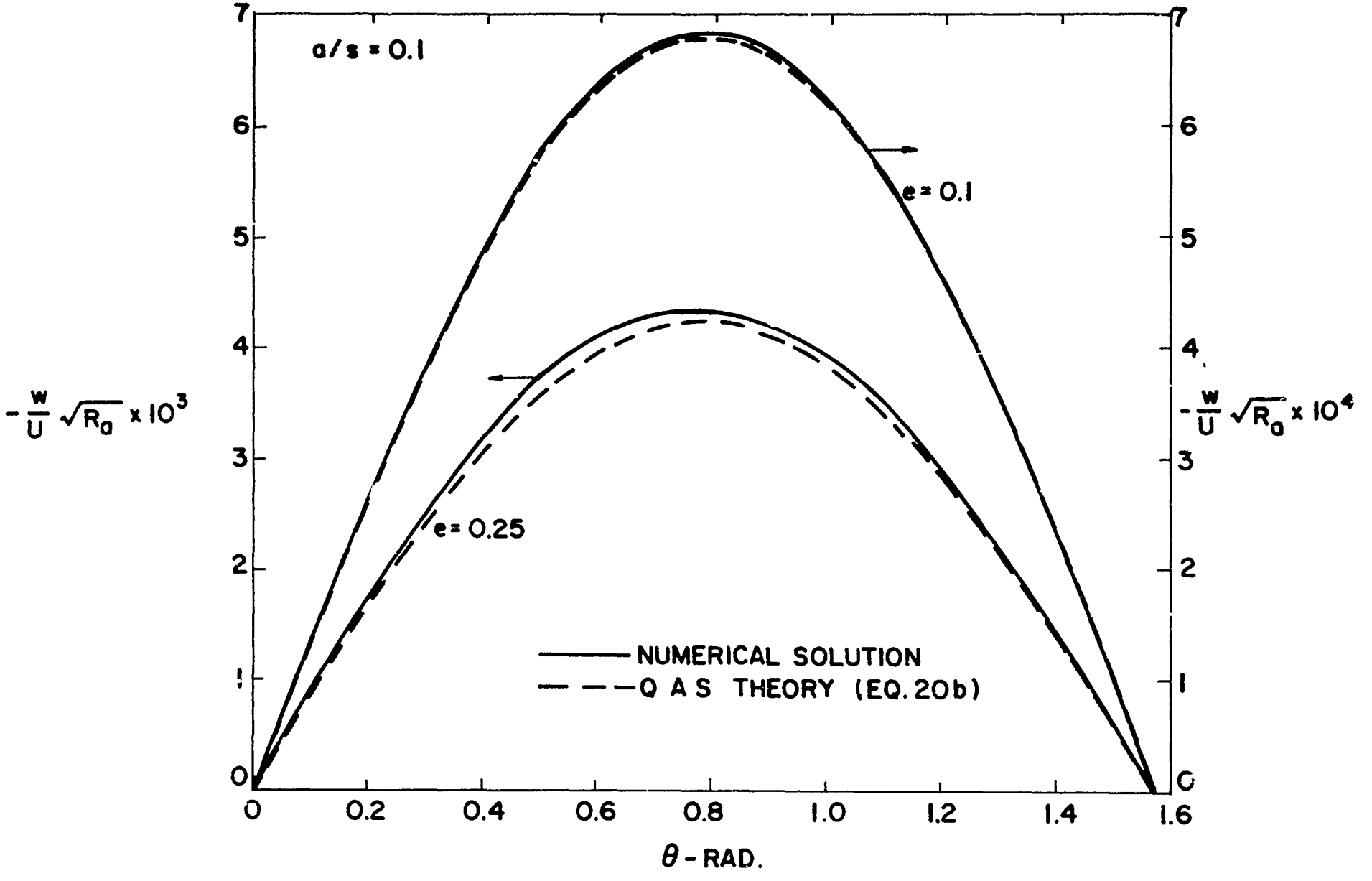

FIG. 7 CROSS FLOW: Q A S THEORY